Catalysis Today xxx (xxxx) xxx–xxx

Contents lists available at ScienceDirect

Catalysis Today

journal homepage: www.elsevier.com/locate/cattod

Optimizing the performance of porous pyridinium frameworks for carbon dioxide transformation

Yanpei Song[a], Qi Sun[b,*], Briana Aguila[a], Shengqian Ma[a,*]

[a] Department of Chemistry, University of South Florida, 4202 E. Fowler Avenue, Tampa, FL, 33620, United States
[b] College of Chemical and Biological Engineering, Zhejiang University, Hangzhou, 310027, China

ARTICLE INFO

Keywords:
CO_2 transformation
CO_2 activation
Porous organic polymer
Organocatalysis
Porous ionic polymer

ABSTRACT

Multifunctional catalysts derived from the integration of discrete catalytic partners in a confined space represent an important approach to emulate some of the design philosophies of enzymes. In an effort to design concepts for highly active catalysts for CO_2 transformations, we synthesize and contrast the performance of two porous pyridinium frameworks. The activity is found to be significantly amplified by the introduction of the amine group on the *ortho* position of the pyridinium moieties. The resulting catalyst is capable of highly active and selective cycloaddition of aziridines with CO_2 to 5-substituted-2-oxazolidinone, even under ambient conditions (1 bar, 22 °C). Its high activity originates from CO_2 activation by the pendant amine group in the vicinity of the active species, which facilitates the subsequent catalytic steps.

1. Introduction

Carbon dioxide is a globally available and nontoxic carbon source in the chemists' toolbox [1–9]. The utilization of CO_2 as a starting material to integrate into value-added products is of practical significance and also supports a carbon-neutral cycle that mitigates the intermittency of renewable energy sources [10–13]. A number of pioneering studies on the catalytic transformations of CO_2 have been undertaken in recent years. In particular, the formation of five-membered heterocycles, such as oxazolidinones from aziridines and CO_2, has received considerable attention due to their prevalence as chiral auxiliaries and as biologically active pharmaceutical agents [14–18]. Most efforts in catalytic systems design for such transformations have been focused on metal-based homogeneous catalysts, including metal complexes and alkali metal halides, all of which exhibit high catalytic activity and selectivity [19–21]. Organocatalysts are gaining traction as they are often more cost-effective and sustainable than metal-containing complexes, prompting an ongoing effort for commercialization, despite their molecular nature [22–27]. At large scale, however, heterogeneous processes are clearly desirable [28–31].

In designing a heterogeneous catalyst for the cycloaddition of aziridines and CO_2, we focused our attention on the general proposed catalytic cycle: (1) reactant (aziridines or CO_2) activation, (2) attack by halide anions, and (3) ring closing and extrusion [32–34]. Given the irreplaceable role of the halide anions in the proposed CO_2 insertion step, we identified the reactant's activator as the modifiable component. One recurring motif that was found to be effective was the presence of amine groups, favoring the activation of CO_2 [35]. We surmised that the integration of the amine group within a cationic framework with a halide as counter anion would improve activity. Whereby the proximity and spatial distribution of the catalytic components to satisfy the requisite geometry are essential to maximize potential cooperation. To fulfill this task, we were motivated by the exploration of porous organic polymers (POPs) due to their tunability, allowing one to control, with high fidelity, the composition of the resulting materials, which are desirable properties for catalytic material design [36–50]. Other innate features of this class of materials that we deemed favorable for catalysis were its high hydrothermal and chemical stability, as well as large surface area for ready diffusion of reaction species.

To explore the validity of this concept, herein, we chose pyridinium as the cation building unit, given its amenable synthesis and easy-to-get properties. To set the proximity between the catalytic partners, we arrange them on a single molecule to be used as a monomer for material synthesis. It is shown the performance of the bromine counter anions can be greatly amplified after the introduction of an amine group on the pyridinium unit, leading to a 7.8-fold acceleration in the cycloaddition of aziridines and CO_2 over the control material without the amino substitution. Moreover, we reveal that the basicity of the amine group is the key to promote CO_2 activation and thereby the overall efficiency.

* Corresponding authors.
E-mail addresses: sunqichs@zju.edu.cn (Q. Sun), sqma@usf.edu (S. Ma).

https://doi.org/10.1016/j.cattod.2020.01.031
Received 20 July 2019; Received in revised form 16 January 2020; Accepted 24 January 2020
0920-5861/

Regardless of the specifics, these findings point to an appealing approach for modulating the properties of POPs for catalytic transformations and related applications.

2. Experimental

2.1. Materials

All commercially available chemicals were purchased in high quality and used without further treatment.

2.2. Catalyst preparation

2.2.1. Synthesis of PQA-NH_2Py-Br

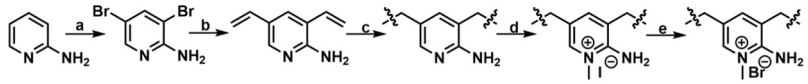

Reagents: (a) NBS; (b) potassium vinyltrifluoroborate, $Pd(PPh_3)_4$; (c) AIBN; (d) CH_3I; (e) NaBr

2.2.1.1. Synthesis of POP-NH_2Py. As a typical procedure, 3,5-divinylpyridin-2-amine (1.0 g) was dissolved in dimethylformamide (DMF, 10 mL), followed by the addition of azobisisobutyronitrile (AIBN, 50 mg). After stirring at room temperature to achieve homogeneity, the mixture was transferred into a 20 mL autoclave and heated to 100 °C overnight, yielding a monolithic light yellow solid. The title product was achieved after washing with acetone and drying under vacuum. 3,5-Divinylpyridin-2-amine was synthesized as follows: 3,5-dibromopyridin-2-amine (2.0 g, 8 mmol), potassium vinyltrifluoroborate (2.64 g, 19.2 mmol), K_2CO_3 (3.2 g, 24 mmol), and $Pd(PPh_3)_4$ (0.232 g, 0.2 mmol) were dissolved in a mixture of toluene (25 mL), THF (25 mL), and H_2O (10 mL), and the resulting mixture was refluxed at 90 °C under N_2 atmosphere for 48 h. The product was extracted with ethyl acetate, washed with brine, dried over Na_2SO_4, and evaporated under reduced pressure, giving the crude compound which was then purified by flash chromatography with hexane/ethyl acetate (2:1) and 1 %v/v triethylamine as eluent to afford the title compound as a yellow powder. ^{1}H NMR (400 MHz, $CDCl_3$, 298 K, TMS): δ 7.98 (d, 1H, J = 1.6 Hz), 7.56 (d, 1H, J = 2.0 Hz), 6.53–6.64 (m, 2 H), 5.56–5.68 (m, 2 H), 5.10–5.40 (m, 2 H), 4.65 (s, 2 H). ^{13}C NMR (100 MHz, $CDCl_3$) δ 155.34, 146.25, 133.38, 131.79, 131.70, 124.84, 118.33, 117.65, 111.72 ppm. 3,5-Dibromopyridin-2-amine was synthesized as follows: 2-aminopyridine (3.76 g, 40 mmol) and *N*-bromosuccinimide (14.24 g, 80 mmol) were added to carbon tetrachloride (80 mL) and stirred at room temperature for 24 h. The product was extracted with chloroform, washed with brine, dried over Na_2SO_4, and evaporated under reduced pressure, giving the crude compound which was then purified by flash chromatography with hexane/ethyl acetate (2:1) and 1 %v/v triethylamine as eluent to afford 3,5-dibromopyridin-2-amine as a yellow powder. ^{1}H NMR (400 MHz, d_6-DMSO, 298 K, TMS): δ 7.27 (d, 1H, J = 8.4 Hz), 7.02 (d, 1H, J = 8.8 Hz), 5.69 (s, 2 H) ppm. The purity of the synthesized compounds was confirmed by NMR analyses (Fig. S1).

2.2.1.2. Synthesis of PQA-NH_2Py-Br. POP-NH_2Py (0.5 g) was swelled in acetonitrile (40 mL), followed by the addition of iodomethane (1.0 g). The mixture was then stirred and heated to 80 °C for 72 h. The resulting powder was washed with ethanol and then exchanged with 1 M NaBr solution three times to afford the title product as a light yellow powder. Elemental analyses reveal that the content of Br species in PQA-NH_2Py-Br is 30.3 wt.%.

2.2.2. Synthesis of PQA-Py-Br

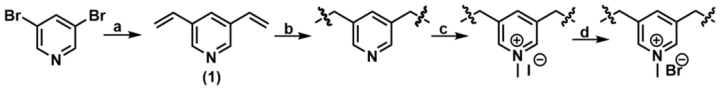

Reagent: (a) potassium vinyltrifluoroborate, $Pd(PPh_3)_4$; (b) AIBN; (c) CH_3I; (d) NaBr

POP-Py (0.5 g), which was synthesized according to the previous literature [51], was swelled in acetonitrile (40 mL), followed by addition of iodomethane (1.0 g). The mixture was then stirred and heated to 80 °C for 72 h. The resulting powder was washed with ethanol and then exchanged with 1 M NaBr solution three times to afford the title product as a light yellow powder. The Brunauer-Emmett-Teller (BET) surface areas of POP-Py and PQA-Py-I are 979 and 465 $m^2 g^{-1}$,

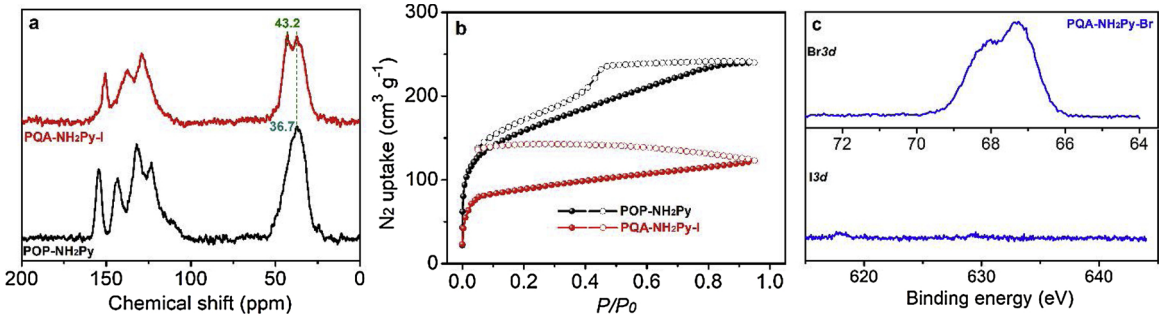

Fig. 1. (a) Solid-state ^{13}C NMR spectra; (b) N_2 sorption isotherms collected at −196 °C; (c) Br*3d* and I*3d* XPS spectra.

respectively. Elemental analyses reveal that the content of Br species in PQA-Py-Br is 33.4 wt.%.

2.3. Catalytic tests

In a typical experimental procedure for coupling of aziridines with CO_2, 1 mmol of aziridine and 5 mg of catalyst were added into a 7 mL vial. After that, the vial was transferred into a 100 mL stainless steel autoclave, sealed, and purged with CO_2. Following this, the pressure of CO_2 was adjusted to the desired value and the autoclave was placed in a preheated oil bath with stirring for the mentioned time period. On completion of the reaction, the reactor was cooled to room temperature and CO_2 was ejected slowly. The conversion and selectivity of the reactions were determined by ^{1}H NMR using terephthalaldehyde as an internal standard. The aziridine compounds were synthesized according to the literature [32].

For recycling the catalyst, the polymer was separated by centrifugation after the reaction, washed with DMF, H_2O, methanol, and hexane in sequence and dried under vacuum, which was used directly for the next catalytic reaction.

2.4. Characterization

Liquid NMR spectra were recorded on a Bruker Avance-400 (400 MHz) spectrometer in which the chemical shifts are expressed in ppm downfield from TMS at $\delta = 0$ ppm, and J values are given in Hz. ^{13}C (100.5 MHz) cross-polarization magic-angle spinning (CP-MAS) solid-state NMR experiments were recorded on a Varian infinity plus 400 spectrometer equipped with a magic-angle spin probe in a 4-mm ZrO_2 rotor. Nitrogen sorption isotherms were measured using Micromeritics ASAP 2020 M and Tristar system, and before the measurements, the samples were degassed at 100 °C for 10 h. IR spectra were recorded on a Nicolet Impact 410 FTIR spectrometer. X-ray photoelectron spectroscopy (XPS) spectra were performed on a Thermo ESCALAB 250 with Al Kα irradiation at $\theta = 90^\circ$ for X-ray sources, and the binding energies were calibrated using the C1s peak at 284.9 eV. Scanning electron microscopy (SEM) images were collected on a Hitachi SU 8000. Elemental analyses were performed via flask combustion followed by ion chromatography.

3. Results and discussion

3.1. Catalyst synthesis

To target the desired materials, we first constructed various pyridine moieties into porous frameworks by polymerization of the corresponding vinyl-functionalized monomers under solvothermal conditions in DMF at 100 °C with the assistance of AIBN. Further treatment of the obtained material (POP-Py and POP-NH_2Py) with methyl iodide (CH_3I), heated to 80 °C for three days gave the porous quaternary ammonium (PQA) salt PQA-Py-I and PQA-NH_2Py-I, respectively. Here, POP-NH_2Py and the corresponding ionic product PQA-NH_2Py-I were selected for thorough illustration. The local structures of these materials were elaborated by solid-state ^{13}C NMR spectroscopy. The successful transformation from the vinyl-functionalized monomers into the highly polymerized polymer is verified by the disappearance of the characteristic vinyl ^{13}C resonance located in the range of 100.0–110.0 ppm with the concomitant emergence of an intense peak at 36.7 ppm attributable to the polymerized vinyl groups. In addition, the appearance of a peak at 43.2 ppm, ascribed to the methyl group in the pyridinium moiety, is indicative of the occurrence of the quaternization reaction (Fig. 1a) [51]. The morphology of POP-NH_2Py and PQA-NH_2Py-I was examined by SEM technique, revealing no noticeable changes after the postsynthetic modification. Both materials feature aggregates comprising interconnected irregular nanoparticles (Fig. S2). Nitrogen sorption measurements collected at 77 K indicate that POP-NH_2Py and PQA-NH_2Py-I are highly porous with BET surface areas of 555 and 310 $m^2 g^{-1}$, respectively (Fig. 1b). The decreased surface area can be reasonably ascribed to the increased mass after the functionality addition. The full accessibility of ionic sites within PQA-NH_2Py-I is indicated by a complete anion-exchange process between I- and Br-, which is supported by the XPS analyses (Fig. 3c). To quantify the content of bromine species in PQA-NH_2Py-Br, elemental analyses were performed, revealing that the weight percentage of bromine species in PQA-NH_2Py-Br was 30.3 wt.%, which corresponds to 92 % of the pyridine moieties participated in the quaternization reaction.

3.2. Catalytic evaluation

The performance of various catalysts were tested for the conversion of 1-butyl-2-phenyl aziridine into 2-oxazolidinones at 50 °C and 2 MPa CO_2 pressure under solvent-free condition with the results presented in Table 1. 5-Aryl-2-oxazolidinone (1) was preferentially formed with high regioselectivities in all cases, indicative of the insertion of CO_2 at the more sterically hindered side of the aziridine. PQA-NH_2Py-Br exhibited much higher reactivity than PQA-Py-Br, inducing a 1-butyl-2-phenyl aziridine conversion of 87 % after 5 h, whereby, PQA-Py-Br only afforded a conversion of 26 % under otherwise identical conditions (Table 1, entries 1 and 2), thus suggestive of an important role of the amine group in catalysis.

To further prove the efficiency of PQA-NH_2Py-Br, kinetic studies were performed at 22 °C and 50 °C (T). As shown in Fig. 2a, the conversions at both temperatures steadily increase over time, following a first-order reaction with rate constants (k) of 0.1592 s^{-1} and 0.2463 s^{-1} for 22 °C and 50 °C, respectively (Fig. 2b). By contrast, PQA-Py-Br afforded the corresponding values of 0.02005 s^{-1} and 0.0609 s^{-1}, with rate constants smaller than those of PQA-NH_2Py-Br by factors of 8 and 4, respectively (Fig. 2c and d). To gain more insight into the reaction, the apparent activation energies were further calculated using Eq. (1), with PQA-Py-Br demonstrating an apparent activation energy (E_A) 2.5 times higher than that for PQA-NH_2Py-Br (31.6 vs. 12.3 kJ mol^{-1}), thus confirming the benefit of incorporating the amine group for catalysis.

$$\ln\left(\frac{k_2}{k_1}\right) = -\frac{E_A}{R}\left(\frac{1}{T_2} - \frac{1}{T_1}\right) \quad (1)$$

To ascertain whether the pendant amine group would also be catalytically active, POP-NH_2Py, POP-Py, and aniline were tested as catalysts. However, all of them were devoid of catalytic activity, under the conditions listed in Table 1, indicating that the Br^- ions are essential for catalysis and the primary amine in PQA-NH_2Py-Br only has a minimal contribution on the reaction outcomes (Table 1, entries 3–5). To further understand the origin of the enhancement of amine substituted pyridinium, a set of control experiments was carried out. Adding free aniline or 2-aminopyridine with PQA-Py-Br gave little improvement in activity, suggesting that the relative position of the amine groups is vital for the improvement of the reactivity, with location at the *ortho* position within a pyridinium framework being crucial. Treating PQA-NH_2Py-Br with 1 M of HBr aqueous solution to neutralize the amine groups, the activity was drastically reduced by a factor of 3.7, close to that of PQA-Py-Br, suggestive of the importance of the basicity of the amine group on the reaction (Table 1, entries 6–10). The basicity of aromatic amines is not strong enough to activate CO_2, but incorporation of them into porous materials increases the capability of CO_2 activation due to the enriched CO_2. To shed additional light on this, we compared the volumetric CO_2 adsorption capacity, and the IR spectra of the pristine and CO_2 reacted samples. PQA-NH_2Py-Br exhibited a bigger Qst value, particularly at the high pressure region, indicative of its higher affinity towards CO_2 (Figs. 3a and S3). In addition, the CO_2 treated PQA-NH_2Py-Br showed an increased intensity at 1650 cm^{-1}, attributable to the carbamic salt, while, no noticeable change was observed for PQA-Py-Br before and after CO_2 treatment

Table 1
Cycloaddition of 1-butyl-2-phenyl aziridine with CO_2 into oxazolidinone over various catalysts.[a].

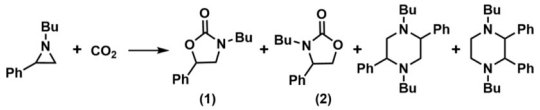

Entry	Catalyst	Time (h)	T (°C)	P (MPa)	Conv. (%)[b]	Select. (%)[b]	Regioselect. (%)/1:2[b]
1	PQA-NH_2Py-Br	5	50	2.0	87	>99	98:2
2	PQA-Py-Br	5	50	2.0	26	>99	98:2
3	POP-NH_2Py	4	70	2.0	9	>99	>99
4	POP-Py	4	70	2.0	6	83	>99
5[c]	aniline	4	70	2.0	7	>99	>99
6	PQA-Py-Br	2	50	2.0	11	>99	>99
7	PQA-NH_2Py-Br	2	50	2.0	37	>99	>99
8[c]	PQA-Py-Br + aniline	2	50	2.0	11	>99	>99
9[c]	PQA-Py-Br +2-aminopyridine	2	50	2.0	11	>99	>99
10	PQA-NH_2Py-Br + HBr	2	50	2.0	10	>99	>99
11	PQA-Py-Br	12	22	0.1	4	>99	>99
12	PQA-NH_2Py-Br	12	22	0.1	31	>99	>99
13	PQA-NH_2Py-Br	72	22	0.1	92	>99	>99
14	PQA-NH_2Py-Br	4	70	2.0	>99	>99	98:2
15[d]	PQA-NH_2Py-Br	4	70	2.0	>99	>99	98:2
16[e]	PQA-NH_2Py-Br	4	70	2.0	>99	>99	98:2

[a] Reaction conditions: 1-butyl-2-phenyl aziridine (1 mmol) and catalyst (5 mg).
[b] The conversion and selectivity of the reactions were determined by ^{1}H NMR using terephthalaldehyde as an internal standard; Select.(%) means the selectivity of oxazolidinone product in the cycloaddition of aziridines with CO_2.
[c] 5 mg of given additive was introduced.
[d] Reuse.
[e] Recycled for 5 times.

(Figs. 3b and S4) [32,33]. To further probe the pendant base effect on the reaction, we contrasted the performance of PQA-NH_2Py-Br and PQA-Py-Br under 1 atm of CO_2 and room temperature, with the aim of increasing the influence of CO_2. As expected, their discrepancy in activity was further increased, affording a 1-butyl-2-phenyl aziridine conversion of 4 % and 31 % for PQA-Py-Br and PQA-NH_2Py-Br, respectively, corresponding to an improvement factor from ca. 3.3–7.8 (Table 1, entries 1, 2, and 11–13).

On the basis of the results described above and previous reports [32–34], we propose a tentative mechanism for the PQA-NH_2Py-Br

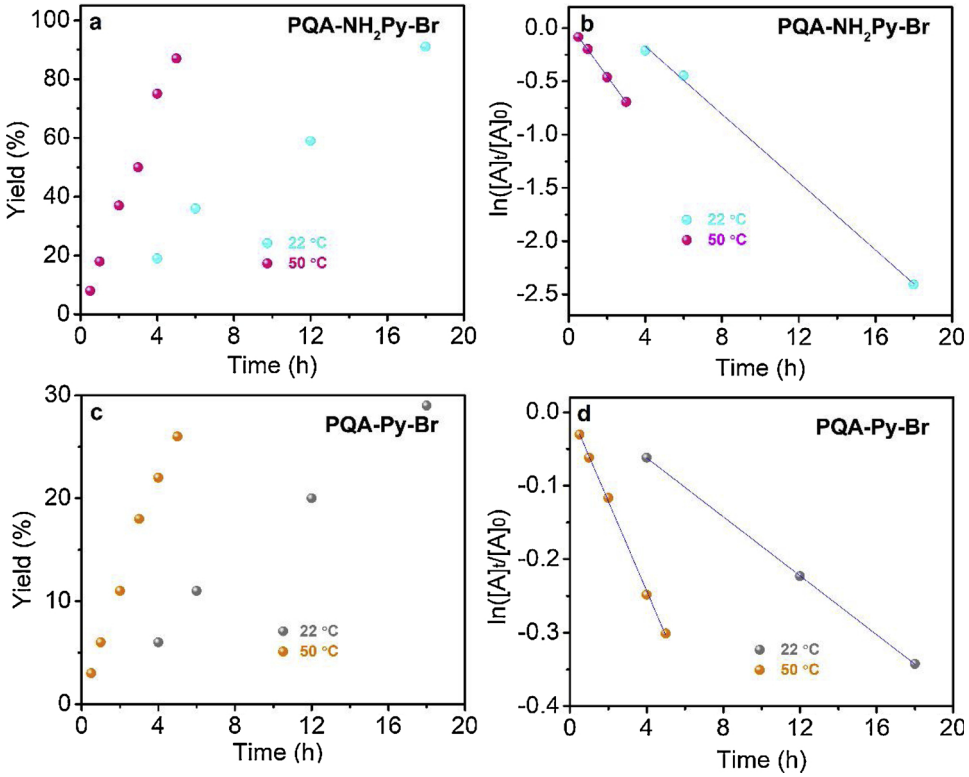

Fig. 2. (a,c) Kinetic rates of 1-butyl-2-phenyl aziridine conversion. (b,d) First order reaction rate plots (R^2>0.99 for all), in which $[A]_0$ is the initial mole concentration of A and $[A]_t$ is the mole concentration of A at the time of t.

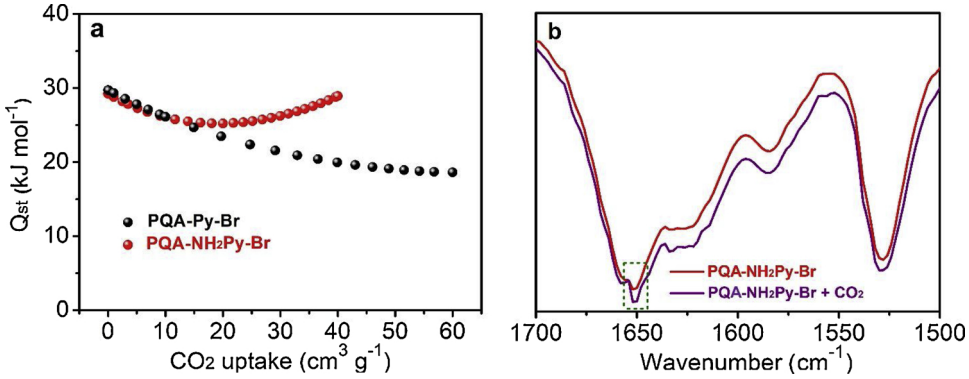

Fig. 3. (a) Isosteric heat of adsorption (Qst) for the adsorption of CO_2 of PQA-Py-Br and PQA-NH_2Py-Br. (b) IR spectra of PQA-NH_2Py-Br before and after treatment with CO_2.

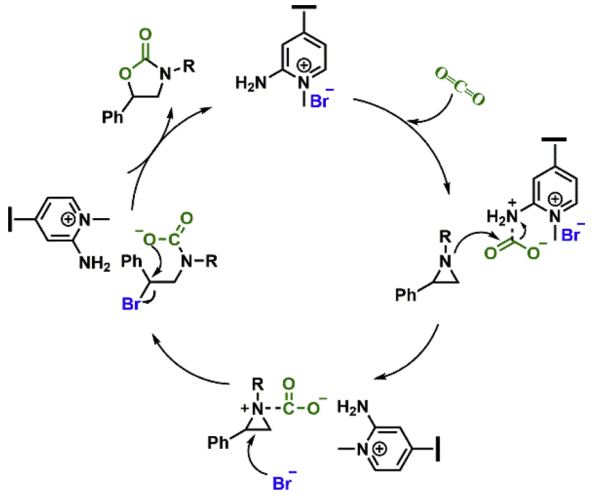

Fig. 4. Proposed mechanism for the PQA-NH_2Py-Br catalyzed cycloaddition of aziridine with CO_2.

catalyzed cycloaddition of aziridine with CO_2 (Fig. 4). Firstly, the substrate and CO_2 are enriched in the porous material, whereby the amine group coordinates reversibly with CO_2 to afford the carbamate salt, which rationalizes the dependence of the reaction rate on CO_2 pressure. The attack of the aziridine substrate on the activated CO_2 carbon generates a positive charge center. Subsequently, the nucleophilic attack of the Br^- ion leads to ring opening of the aziridine through two different pathways, thus giving rise to different regioselectivities. Following this, cyclization via an intramolecular nucleophilic attack leading to oxazolidinones and regeneration of the catalyst. The main product 2-oxazolidinones originates from ring-opening of the aziridine at the most substituted carbon as this produced the more stable carbamate salt.

Having proven the efficiency of PQA-NH_2Py-Br, the reaction conditions were further optimized. 1-Butyl-2-phenyl aziridine was again used as a substrate, while the catalyst loading, reaction temperature, and CO_2 pressure were varied. When the temperature increased to 70 °C with 2 MPa of CO_2, full conversion of 1-butyl-2-phenyl aziridine can be achieved within 4 h (Table 1, entry 14). Reducing the catalyst loading to 0.01 mol %, and under otherwise identical conditions the yield of 5-aryl-2-oxazolidinone exceeded 99 % after 48 h, which corresponds to a turnover number TON, measured as total moles of product per mole of catalyst of 10,000. When the pressure and temperature were decreased to 1 bar and 22 °C, respectively, PQA-NH_2Py-Br was still efficient, and 92 % conversion of 1-butyl-2-phenyl aziridine to oxazolidinone was achieved after 72 h. Moreover, PQA-NH_2Py-Br could be filtered and reused without loss of activity after 5 recycles (Table 1, entries 15 and 16, and Table S1).

Encouraged by this, we further investigated its generality in the cycloaddition reactions of CO_2 with various aziridines (Table S2). It was found that the reaction of 2-phenylaziridine proceeded smoothly with excellent yield achieved within 4 h. The substrate bearing a branched alkyl group at the nitrogen atom showed a slower reaction rate and a relatively low selectivity probably due to the steric interactions as well as the formation of self-oligomers. The rate dependence on the steric effect of the R group on the nitrogen atom implies that the coordination of CO_2 to the aziridine is a reversible step in the catalytic cycle. The substrates with less sterically hindered R would be favorable for the coordination with CO_2, thus resulting in higher reaction rate compared with those substrates with more sterically hindered R. These results further support our catalyst design concept that the introduction of the amine group favorable for the CO_2 coordination could promote the reaction.

4. Conclusion

In summary, we have developed two new catalysts for CO_2 transformation, and our results are significant in demonstrating new design principles to enhance reaction rates under mild conditions. Incorporating an amine group at the *ortho* position of the pyridinium framework increases activity by almost an order of magnitude. Based on experimental studies, the origin of the rate enhancement is believed to be primarily due to the presence of a pendant base in the proximity of active sites, promoting the CO_2 activation. Ongoing work in our laboratories is focused on extending such catalyst design concept to other CO_2 related transformations, and the results will be reported separately in due course.

Declaration of Competing Interest

The authors declare that they have no known competing financial interests or personal relationships that could have appeared to influence the work reported in this paper.

CRediT authorship contribution statement

Yanpei Song: Data curation, Investigation, Writing - original draft, Validation. **Qi Sun:** Writing - review & editing, Methodology, Formal analysis. **Briana Aguila:** Writing - review & editing. **Shengqian Ma:** Conceptualization, Supervision, Resources, Project administration.

Acknowledgment

The authors acknowledge the University of South Florida for financial support of this work.

Appendix A. Supplementary data

Supplementary material related to this article can be found, in the online version, at doi:https://doi.org/10.1016/j.cattod.2020.01.031.

References

[1] H. He, J.A. Perman, G. Zhu, S. Ma, Small 12 (2016) 6309–6324.
[2] A.M. Appel, J.E. Bercaw, A.B. Bocarsly, H. Dobbek, D.L. DuBois, M. Dupuis, J.G. Ferry, E. Fujita, R. Hille, P.J.A. Kenis, C.A. Kerfeld, R.H. Morris, C.H.F. Peden, A.R. Portis, S.W. Ragsdale, T.B. Rauchfuss, J.N.H. Reek, L.C. Seefeldt, R.K. Thauer, G.L. Waldrop, Chem. Rev. 113 (2013) 6621–6658.
[3] Q. Liu, L. Wu, R. Jackstell, M. Bell, Nat. Commun. 6 (2015) 5933.
[4] Q. Sun, B. Aguila, J.A. Perman, N. Nguyen, S. Ma, J. Am. Chem. Soc. 138 (2016) 15790–15796.
[5] J. Liu, G. Chen, Y. Zhu, Z. Liang, A. Pei, C.-L. Wu, H. Wang, H.R. Lee, K. Liu, S. Chu, Y. Cui, Nat. Catal. 1 (2018) 592–600.
[6] B. Aguila, Q. Sun, X. Wang, E. O'Rourke, A.M. Al-Enizi, A. Nafady, S. Ma, Angew. Chem. Int. Ed. 57 (2018) 10107–10111.
[7] W. Desens, C. Kohrt, M. Frank, T. Werner, ChemSusChem 8 (2015) 3815–3822.
[8] Z. Dai, Q. Sun, X. Liu, C. Bian, Q. Wu, S. Pan, L. Wang, X. Meng, F. Deng, F.-S. Xiao, J. Catal. 338 (2016) 202–209.
[9] J.M. Barlow, J.Y. Yang, A.C.S. Cent, Science 5 (2019) 580–588.
[10] Y. Zhou, F. Che, M. Liu, C. Zou, Z. Liang, P.D. Luna, H. Yuan, J. Li, Z. Wang, H. Xie, H. Li, P. Chen, E. Bladt, R. Quintero-Bermudez, T.-K. Sham, S. Bals, J. Hofkens, D. Sinton, G. Chen, E.H. Sargent, Nat. Chem. 10 (2018) 974–980.
[11] S. Das, F.D. Bobbink, G. Laurenczy, P.J. Dyson, Angew. Chem. Int. Ed. 53 (2014) 12876–12879.
[12] (a) P. Gao, S. Li, X. Bu, S. Dang, Z. Liu, H. Wang, L. Zhong, M. Qiu, C. Yang, J. Cai, W. Wei, Y. Sun, Nat. Chem. 9 (2017) 1019–1024;
(b) Y. Zhao, G.I.N. Waterhouse, G. Chen, X. Xiong, L.-Z. Wu, C.-H. Tung, T. Zhang, Chem. Soc. Rev. 48 (2019) 1972–2010.
[13] H.B. Gray, Nat. Chem. 1 (2009) 7.
[14] H. Xu, X.-F. Liu, C.-S. Cao, B. Zhao, P. Cheng, L.-N. He, Adv. Sci. 3 (2016) 1600048.
[15] M.R. Barbachyn, C.W. Ford, Angew. Chem. Int. Ed. 42 (2003) 2010–2013.
[16] T.M. Makhtar, G.D. Wright, Chem. Rev. 105 (2005) 529–542.
[17] L. Aurelio, R.T.C. Brownlee, A.B. Hughus, Chem. Rev. 104 (2004) 5823–5846.
[18] K.J. Lamb, I.D.V. Ingram, M. North, M. Sengoden, Curr. Green Chem. 6 (2019) 32–43.
[19] A.W. Miller, S.T. Nguyen, Org. Lett. 6 (2004) 2301–2304.
[20] Y. Xie, C. Lu, B. Zhao, Q. Wang, Y. Yao, J. Org. Chem. 84 (2019) 1951–1958.
[21] P. Tascedda, E. Duñach, Chem. Commun. (2000) 449–450.
[22] H.-F. Jiang, J.-W. Ye, C.-R. Qi, L.-B. Huang, Tetrahedron Lett. 51 (2010) 928–932.
[23] R.A. Watile, D.B. Bagal, Y.P. Patil, B.M. Bhanage, Tetrahedron Lett. 52 (2011) 6383–6387.
[24] A.C. Kathalikkattil, J. Tharun, R. Roshan, H.-G. Soek, D.-W. Park, Appl. Catal. A-Gen. 447-448 (2012) 107–114.
[25] J. Seayad, A.M. Seayad, J.K.P. Ng, C.L.L. Chai, ChemCatChem 4 (2012) 774–777.
[26] Y. Du, Y. Wu, A.-H. Liu, L.-N. He, J. Org. Chem. 73 (2008) 4709–4712.
[27] V.B. Saptal, B.M. Bhanage, ChemSusChem 9 (2016) 1980–1985.
[28] X.-Z. Lin, Z.-Z. Yang, L.-N. He, Z.-Y. Yuan, Green Chem. 17 (2015) 795–798.
[29] X. Wang, W.-Y. Gao, Z. Niu, L. Woktas, J.A. Perman, Y.-S. Chen, Z. Li, B. Aguila, S. Ma, Chem. Commun. 54 (2018) 1170–1173.
[30] C.-S. Cao, Y. Shi, H. Xu, B. Zhao, Dalton Trans. 47 (2018) 4545–4553.
[31] C. Qi, J. Ye, W. Zeng, H. Jiang, Adv. Synth. Catal. 352 (2010) 1925–1933.
[32] Z.-Z. Yang, L.-N. He, S.-Y. Peng, A.-H. Liu, Green Chem. 12 (2010) 1850–1854.
[33] H. Zhou, Y.-M. Wang, W.-Z. Zhang, J.-P. Qu, X.-B. Lu, Green Chem. 13 (2011) 644–650.
[34] D. Adhikari, A.W. Miller, M.-H. Baik, S.T. Nguyen, Chem. Sci. 6 (2015) 1293–1300.
[35] D.B. Nale, S. Rana, K. Parida, B.M. Bhanage, Appl. Catal. A-Gen. 469 (2014) 340–349.
[36] Q. Sun, B. Aguila, G. Verma, X. Liu, Z. Dai, F. Deng, X. Meng, F.-S. Xiao, S. Ma, Chem 1 (2016) 628–639.
[37] Q. Sun, Z. Dai, X. Meng, F.-S. Xiao, Chem. Soc. Rev. 44 (2015) 6018–6034.
[38] Q. Sun, Z. Dai, X. Liu, N. Sheng, F. Deng, X. Meng, F.-S. Xiao, J. Am. Chem. Soc. 137 (2015) 5204–5209.
[39] A.G. Slater, A.I. Cooper, Science 348 (2015) aaa988.
[40] S. Das, P. Heasman, T. Ben, S. Qiu, Chem. Rev. 117 (2017) 1515–1563.
[41] Y. Xu, S. Jin, H. Xu, A. Nagai, D. Jiang, Chem. Soc. Rev. 42 (2013) 8012–8031.
[42] D. Wu, F. Xu, B. Sun, R. Fu, H. He, K. Matyjaszewski, Chem. Rev. 112 (2012) 3959–4015.
[43] T. Ben, C. Pei, D. Zhang, J. Xu, F. Deng, X. Jing, S. Qiu, Energy Environ. Sci. 4 (2011) 3991–3999.
[44] Z. Yan, Y. Yuan, Y. Tian, D. Zhang, G. Zhu, Angew. Chem. Int. Ed. 54 (2015) 12733–12737.
[45] P. Wang, Q. Xu, Z. Li, W. Jiang, Q. Jiang, D. Jiang, Adv. Mater. 30 (2018) 1801991.
[46] N. Chaoui, M. Trunk, R. Dawson, J. Schmidt, A. Thomas, Chem. Soc. Rev. 46 (2017) 3302–3321.
[47] W. Wang, C. Li, L. Yan, Y. Wang, M. Jiang, Y. Ding, ACS Catal. 6 (2010) 6091–6100.
[48] X. Wang, Y. Zhou, Z. Guo, G. Chen, J. Li, Y. Shi, Y. Liu, J. Wang, Chem. Sci. 6 (2015) 6916-1924.
[49] X. Yu, Z. Yang, B. Qiu, S. Guo, P. Yang, B. Yu, H. Zhang, Y. Zhao, X. Yang, B. Han, Z. Liu, Angew. Chem. Int. Ed. 58 (2019) 632–636.
[50] Y. Xie, T.-T. Wang, X.-H. Liu, K. Zou, W.-Q. Deng, Nat. Commun. 4 (2013) 1960.
[51] Q. Sun, L. Zhu, B. Aguila, P.K. Thallapally, C. Xu, J. Chen, S. Wang, D. Rogers, S. Ma, Nat. Commun. 10 (2019) 1646.